

CFRP panels' fatigue behavior under varying loads in comparison to their fatigue behavior under constant loading

Fadhil Talib Salman

Enaam Obeid Hassoun

Majida Khaleel Ahmed

*Electromechanical Engineering Department,
University of Technology, Baghdad, Iraq.*

Published on: 6 March 2025



This work is licensed under a
Creative Commons Attribution-
NonCommercial 4.0
International License.

Abstract

Carbon fiber reinforced polymer (CFRP) composites have been extensively utilized in engineering applications for a considerable period, owing to their corrosion resistance, high stiffness, and exceptional lightness. Nonetheless, the loads that materials, particularly composites, encounter render them susceptible to collapse or the accumulation of damage, ultimately resulting in complete failure at some stage, regardless of whether these loads are fixed or variable. Consequently, enhancing the internal structure design of carbon fiber-reinforced polymer composites to suit various applications is critically important. This study investigates the failure behavior of CFRP laminates under static loads for one specimen

and variable loads using a regular low-cycle fatigue (LCF) procedure for another, as well as a low-cycle (varying) fatigue procedure from low to high stresses and vice versa, for two other specimens. Under the same load limits for all tests without reaching the stage of complete failure of the specimen. The experimental procedure involved the use of a specially designed apparatus to apply loads through internal air pressure to the center of the panel once it was securely fixed in place. The observed deformation of the specimen was tracked in line with its maximum deflection measurements. The experimental results were compared to the theoretical maximum deflection under static loading. To ensure that the experimental and theoretical results are consistent to

the extent that allows periodic fatigue tests according to correct measurements and building on them. The study showed that CFRP sheets are exposed to minimal deformation under static loads, where the maximum deflection reached (5.94 mm) compared to the uniform low-cycle fatigue loads, which recorded a higher deformation at a deflection of (6.16 mm). In contrast, the varying low-cycle fatigue loads were more harmful to the internal structure of (CFRP) sheets until the maximum deflection was reached and at the same limits (7.91 mm) in low to high pressure. In comparison, it came (8.51 mm) at high to low pressure, indicating a large deformation of the sample when it is under varying pressures.

Keywords: Carbon Fiber Reinforced Polymer (CFRP), Accumulation of damage, Static Loading, Low-Cycle Fatigue, (LCF), low-cycle (varying) fatigue

* INTRODUCTION

Composites are made up of two or more micro-constituents that work together but have different chemical and physical properties.

The point of using many components is to capitalize on their combined strengths while avoiding the drawbacks of any one of them.

1- Rapid industrial expansion necessitates materials that exhibit enhanced strength, stiffness, density, cost-effectiveness, and sustainability. Composites exhibit comparable characteristics. In numerous applications, polymers have supplanted metals in recent decades.

2- CFRP composites have a low coefficient of thermal expansion, high specific strength, stiffness, and toughness, as well as self-lubricating ability, so carbon/carbon composites are frequently used in aerospace and aerospace industries for structural and frictional applications as well as brake materials for high-speed vehicles.

3,4- A robust association exists between the microstructure of carbon fiber and its physical properties;

imperfections in the fiber, carbon concentration, and the orientation of graphite structure all influence the fibers' modulus of elasticity, strength, and electrical conductivity.

5- Even with the ongoing expansion of the application of laminated composite structures, issues like delamination and micro-cracking continue to pose significant challenges, particularly in the context of aerospace structures.

6- Their great strength, stiffness, impact resistance, and lightweight

make them popular in these and other applications. However, weak matrix-fiber interfaces in fiber-reinforced polymers CFRP frequently cause disbands and crack-like flaws during manufacturing and service. Thus, fracture initiation and development from such faults under diverse loading situations and speeds is possible. Therefore, knowing the processes that influence CFRP fracture behaviors under varied loading rates is essential for quantifying significant technical parameters and failure characteristics. Several studies have examined polymer composite fracture behavior under quasi-static and dynamic (impact) stresses.

7,8,9- Under static loading circumstances, the extent of deformation progressively escalates with the rise in load. The fiber will persist in deforming until its strength is entirely depleted.

10- It is widely understood that CFRP composites are routinely subjected to tension fatigue stress in engineering structures, which results in irreparable damage and a significant drop in service performance. Furthermore, compared to aviation or aerospace structures, civil engineering has a substantially longer service life and works in a more complex environment

11,12- CFRP's inhomogeneity complicates fatigue failure analysis. Fatigue refers to the increasing damage resulting from repetitive cyclic loads. Continuous cyclic loading can cause material damage even at stress levels significantly below the elastic limit; in addition, the extent of fatigue damage varies significantly between low-cycle fatigue and high-cycle fatigue. In CFRP, both low-cycle fatigue and high-stress result in irreparable harm. Conversely, in high-cycle fatigue situations, the stress levels are sufficiently low to keep the material within its elastic ratio constraints. This leads to the gradual degradation of composites over time.

13- There is a substantial relationship between the fatigue performance of carbon fiber-reinforced plastic (CFRP) and the specimen geometry and material properties, which include fiber volume fractions, orientation, and thickness. Johri et al. (2021)

14- The fatigue performance of CFRP composites is notably affected by fatigue load spectrums and environmental factors. Vieille et al. (2014)

15- It was found that Nano-voids and cavitation around Nano-particles serve as the primary damage locations within the matrix and that

the point of crack initiation corresponds with a region of elevated stress. Capela et al. (2019) 16- Voids and porosity represent significant challenges in the manufacturing process. Voids and porosity differ in terms of pore size. A void typically refers to a large pore, while porosity denotes a collection of small pores; however, in industrial contexts, these terms are often used interchangeably. Voids may develop in the ply interfaces or within the individual plies. Uusitalo, K. (2013)

17- Estimating fatigue life for composite is challenging due to variations in fibers, matrix, lamination stacking sequence, production techniques, and other influencing factors. Fatigue life in composites cannot be modeled or predicted in the same manner as it is for metals and traditional materials. The reason is The disparity in fatigue behavior between metals and composites. Vassilopoulos & Keller (2011)

18- To accurately predict the fatigue life of composites subjected to different loads, it is essential to comprehend the behavior of alternating and mean stresses in the context of constant amplitude loading and their implications. Conducting fatigue testing under various cyclic loading conditions is essential to

assess the influence of loading modes on the fatigue sensitivity of composites. The approach requires both time-intensive and costly work. Uusitalo, K. (2013) [17] Vassilopoulos categorizes tiredness behavior theories into two groups. Initially, theories are based on macroscopic failure criteria and formulae to forecast life under constant or changing amplitude loading. Those hypotheses ignore damage mechanism experiments and fatigue development. S-N curves and computational models are examples of such theories. Theories in the second category are that the damage metric is employed to indicate damage buildup in theories based on fatigue life damage assessments. The metric divides these theories into strength degradation fatigue, stiffness degradation fatigue, and actual damage mechanism fatigue theories. Vassilopoulos (2010)

19- In elastic theory, the deformation of circular plates poses considerable challenges. Circular plates find utility in various technical applications. This topic has garnered considerable interest over an extended period. Calculating deflections and bending moments in thin circular elastic plates subjected to uniform loads or internal pressures can significantly improve the design and analysis of structural

elements or systems. Uusitalo, K. (2013) [17] The differential equations of an appropriate plate theory ascertain deflection. This deflection serves as an estimate of the stress experienced by the plate. Stresses serve as indicators for potential plate failure when subjected to load in failure theories. Mojahedin et al. (2016)

20- This paper presents an experimental study of the effect of constant loads, uniform low-cycle fatigue loads, and low-cycle fatigue with varying stressors from low to high and high to low, all within the same range of applied pressures. For all tests of carbon fiber-reinforced polymer sheets with the same thickness, the experimental results taken from a device designed for this purpose are compared with the theoretical results, and the maximum deflection values of the sheet are adopted as a criterion for deformation.

* Methodology for experimental procedures

It has two sides: the first is the sample used, and the second is the device designed for the experimental procedure: -

1- The specimen utilized in this experimental study of a 3K (3000 individual strands combined) orthogonal plate CFRP and an epoxy

resin matrix, a thickness of $h = 0.25$ mm (with fiber layers oriented at 45°) and dimensions of 350 x 350 mm, while the cross-section subjected to the transverse load measures 150mm circular diameter.

2- Table (1) shows the mechanical properties of an orthotropic plate of the carbon fiber perpendicular plate after the experimental tensile test, while Table (2) shows the chemical analysis of the sample using the Axia chemiSEM device compared to the results of the American standard.

TABLE 1. Mechanical properties of carbon fiber in an orthotropic context

Parameter	Symbol	Value	Unit
Elastic Modulus in X	E_x	250×10^9	N/m ²
Elastic Modulus in Y	E_y	280×10^9	N/m ²
Elastic Modulus in Z	E_z	280×10^9	N/m ²
Shear modulus in XY	G_{xy}	340×10^9	N/m ²
Shear modulus in YZ	G_{yz}	150×10^9	N/m ²
Shear modulus in XZ	G_{xz}	370×10^9	N/m ²
Poisson's ratio in XY	ν_{xy}	0.38	-
Poisson's ratio in YZ	ν_{yz}	0.3	-
Poisson's ratio in XZ	ν_{xz}	0.3	-
Tensile Strength in X	R_{mX}	750×10^6	N/m ²
Tensile Strength in Y	R_{mY}	1201×10^6	N/m ²
Yield Strength in X	R_{eX}	690×10^6	N/m ²
Yield Strength in Y	R_{eY}	977×10^6	N/m ²
Mass Density	ρ	1790	Kg/m ³

TABLE 2. Analysis of the chemical composition of carbon fiber-reinforced polymer

Type of test	C%	O %	Cl %	Nl %	other
Standard	75	22	0.3	0.1	0.5
Experimental	77.6	21.8	0.4	0.2	0.5

The device was designed according to a system that allows the efficient regulation of internal air pressure from an air compressor, capable of producing a maximum pressure of (1 MPa). The pressure is managed via a manual control valve, enabling accurate modifications within a control range of (0 to 4 MPa). The designated pressure is

subsequently directed to an inlet solenoid valve, which exhibits a closing force varying from (0 to 4 MPa). This valve works on transferring compressed air at the specified time into a test cylinder made of cast iron, featuring a thickness of (5 mm) and a transverse diameter of (150 mm). This design creates a transverse space that is open from the top, serving as a window for the pressure applied uniformly and consistently at the center of the sample, which is securely affixed to the top of the test cylinder. A pressure sensor, capable of sensing from (0 to 4 MPa), is mounted on the cylinder wall to measure the pressure within the test cylinder accurately. A digital displacement disk on top of the cylinder will monitor load-induced sample deformation. This disc will contact the sample's surface through a sensor tube to detect the greatest deviation during deformation with a range of (0 to 26 mm) and an accuracy of (0.01) mm. After the prescribed pressure retention time, the outlet solenoid valve releases the cylinder pressure.

The procedural sequence of the device components is linked by connecting pipes constructed from carbon steel, featuring a thickness of (3.7 mm) and a length of (1200 mm), commencing at the air compressor

and concluding at the outlet solenoid valve. The system is predominantly governed by the control unit, represented by the PLC, which regulates the timing of compressed air entry, its duration within the cylinder, and the expulsion of air from the cylinder. The controller facilitates the repetition of the procedure under identical standards across multiple cycles, with a cycle range of (0 to 999), a timing interval between cycles of (0 to 999) seconds, and a delay in pressure within the cylinder from (0 to 99) seconds. The device can perform both static and fatigue tests that need repeated cycles, such as regular low-cycle fatigue (LCF) as well as low-cycle (varying) fatigue.

The test was conducted at room temperature, with loads incrementally and consistently increased during both the static load test and the low-cycle fatigue test. Additionally, varying loads were applied in the fatigue test at different stress levels. Figure (1) illustrates the experimental system employed in this study. Figure (2) illustrates a schematic representation of the apparatus, detailing the specified components.



FIGURE 1. The utilized experimental system

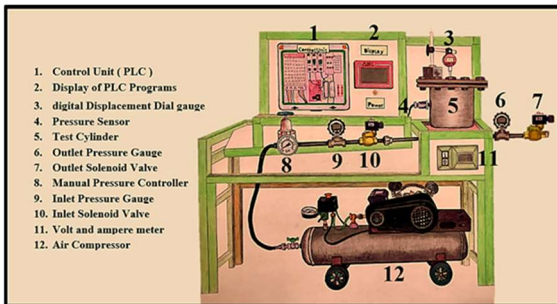


FIGURE 2. the experimental system's schematic diagram.

*** FUNDAMENTAL MATHEMATICAL EQUATIONS FOR UNIFORMLY DISTRIBUTED LOADS**

*** Analysis of Large Deflections in Orthotropic Thin Plates**

It is assumed that the principal axes of the circle's diameter, which is subjected to the applied load, align parallel with the principal directions of the orthotropic material. When an orthotropic circular plate with radius (a) and a uniform applied load (q) is set up with a = b, it is expressed by equation (1). [21]

$$1 - W = \frac{q}{64 D_1} (a^2 - r^2)^2$$

$$2- \text{Where: } r = \sqrt{x^2 + y^2}$$

$$3- D_1 = \frac{1}{8} (3 D_x + 2H + 3 D_y)$$

$$4 - H = D_{xy} + 2G_{xy}$$

$$5- D_{xy} = \frac{t^3 E'_x v_y}{12 (1 - v_x v_y)} = \frac{t^3 E'_y v_x}{12 (1 - v_x v_y)}$$

$$6 - G_{xy} = \frac{r^3 G}{12}$$

$$7 - D_x = \frac{t^3 E'_x}{12 (1 - v_x v_y)}$$

$$8 - D_y = \frac{t^3 E'_y}{12 (1 - v_x v_y)}$$

The stresses that were observed in the center of the composite plate when $r = 0$, regardless of r and θ , can be articulated as follows:

$$9- \sigma_r = \sigma_\theta = \frac{3q}{4} \left[\frac{a}{h} \right]^2$$

The tensile strain at the center of the plate during significant deflections of the composite material may be determined by [22]

$$10- \varepsilon_r = \varepsilon_\theta = 0.462 \frac{w^2}{a^2}$$

The tangential strain (ε_t) and effective strain (ε_{ff}) experienced by the composite plate can be determined using the following equations: [23]

$$11- \varepsilon_t = -[\varepsilon_r + \varepsilon_\theta]$$

$$12- \varepsilon_{eff} = \sqrt{\frac{2}{3} (\varepsilon_r^2 + \varepsilon_\theta^2 + \varepsilon_t^2)}$$

* Mechanical considerations of fatigue fracture

An analysis of stress and strains under cyclic loading is essential for engineering applications. In certain practical applications, the material functions under constant maximum and minimum stress levels. This is referred to as constant amplitude stressing. The mean stress, σ_m , is the average of the maximum σ_{max} and minimum σ_{min} stress values, and the algebraic difference is the difference between the maximum and minimum stress values, $\Delta\sigma = \sigma_{max} - \sigma_{min}$. The half range is referred to as stress amplitude. The following are the mathematical expressions: [24]

$$13- \sigma_m = \frac{\sigma_{max} + \sigma_{min}}{2}$$

$$14- \sigma_a = \frac{\sigma_{max} - \sigma_{min}}{2}$$

The stress ratio R is defined as the ratio of minimum stress to maximal stress and is:

$$15- R = \frac{\sigma_{min}}{\sigma_{max}}$$

Where R=1 denotes the static tensile load.

* Experimental findings comparing the two tests and discussion

Four carbon fiber composite specimens with a uniform thickness of (0.25 mm) were selected for the experimental test. Pressures from 1 bar to the value that does not lead to

complete collapse of the specimens are applied over the diagonal cross-sectional area (150 mm). By means of a disc displacement gauge set at $r = 0$, the maximum deflection values of the specimens are read. After the specimen is placed firmly on the test cylinder, the experimental test is started using the testing mechanism of the specially designed apparatus.

In both the static load test and the fatigue under constant load test, the specimen deformation causes convexity with increasing loads. This deformation is linear, with the deflection values of the fatigue under the constant load being larger than the static loads. The fatigue test mechanism stabilizes the maximum deflection values after several cycles of static loading, which explains this Inequality. Table (3) shows the comparison between the experimental maximum deflection values for static loading compared to the fatigue under constant load under the same limits, while Figure (3) shows the comparison between the maximum deflections for both tests. Figure (4) shows the relationship between the number of cycles in the fatigue under constant load and the maximum deflection for each applied load after a series of cycles; the black colour at the end of each deflection

indicates that the deflection value stabilises after multiple cycles.

TABLE 3. The results of experimental deflections for static load and fatigue under a constant load.

Pressure*10 ⁵ N/m ²	under static load		fatigue under constant load	
	Experimental Max. Deflection mm	After a number of cycles	Experimental Max. Deflection mm	Experimental Max. Deflection mm
1	2.30	27	2.56	
2	3.65	33	3.72	
3	4.84	33	5.06	
4	5.94	29	6.16	

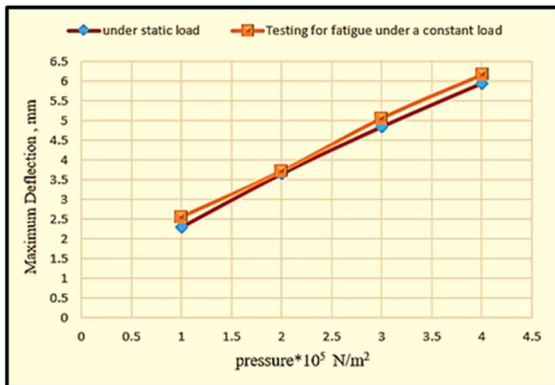


FIGURE 3. The maximum deflection under static load and the fatigue under constant load of CFRP

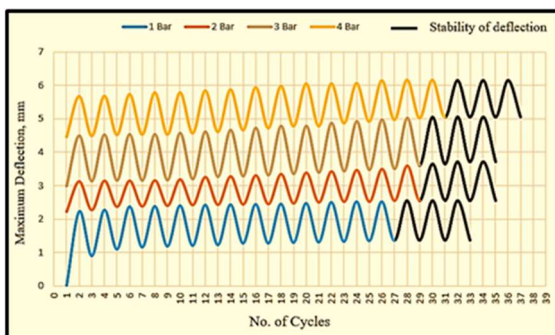


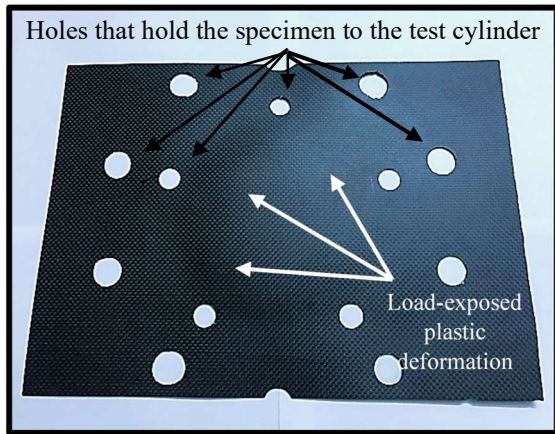
FIGURE 4. The relationship between the number of cycles and the maximum deflection values of the fatigue * under constant load of CFRP

In the fatigue test conducted under variable load conditions, ranging from a low pressure of 1 bar to a high pressure of 4 bar, the sample demonstrated increased deformation before reaching stabilization at maximum deflection after multiple cycles, in contrast to the fatigue test

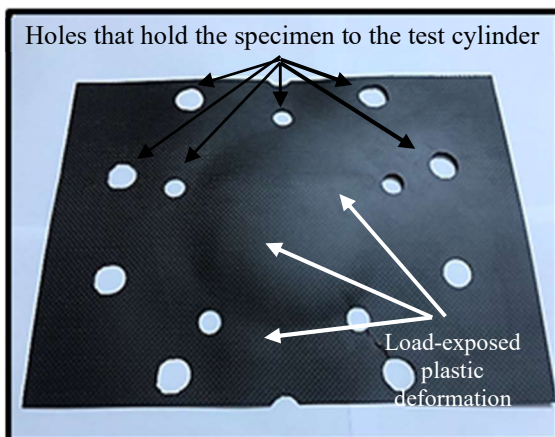
performed under constant load conditions. The notable variation in deformation, when compared to the fatigue testing under constant load, is particularly evident during the initial three cycles. Following this period, the maximum deflection values exhibited a natural increase until they ultimately reached a state of stabilization. The maximum deflection values of the sample subjected to the fatigue test under variable load, ranging from a high pressure of 4 bar to a low pressure of 1 bar, exhibited greater deformation than those observed in both the fatigue testing under constant load and the low-to-high fatigue test. This resulted in a higher deflection value at the conclusion of the cycles. Noting that the first and second cycles recorded the relatively higher deformation values compared to the previous two tests before the deflection values took a predictable gradation until the end of the cycles.

The two samples after fatigue testing under variable load with pressures from 1 to 4 bar and 4 to 1 bar are shown in Figure (5). Table (4) also compares the maximum deflection for each test under static loading, fatigue under constant load the fatigue testing under variable load, and 1 to 4 bar and 4 to 1 bar conditions. Figures (6,7) show the

link between the number of cycles and the maximum deflection in fatigue testing under variable loads from 1 to 4 bar and 4 to 1 bar, respectively.



a- Deformation of the sample under 1 to 4 bar.



b- Deformation of the sample under 4 to 1 bar.

FIGURE 5. The two samples after fatigue testing under variable load

TABLE 4. of the maximum deviations observed across the four tests (Under Static load, Fatigue under constant load, Fatigue under variable load 1 to 4 bar and Fatigue under variable load 4 to 1 bar) At the same applied pressure limits

orthotropic carbon fiber-reinforced polymer			
Pressure $\times 10^6$ N/m ²	Under Static load	Fatigue under constant load	Fatigue under variable load Low to High
	Max. Deflection mm	Max. Deflection mm	Max. Deflection mm
1	2.30	2.53	4.74
4	5.94	6.16	7.91
Pressure $\times 10^6$ N/m ²	Under Static load	Fatigue under constant load	Fatigue under variable load High to Low
	Max. Deflection mm	Max. Deflection mm	Max. Deflection mm
4	5.94	6.16	8.51
1	2.30	2.53	5.44

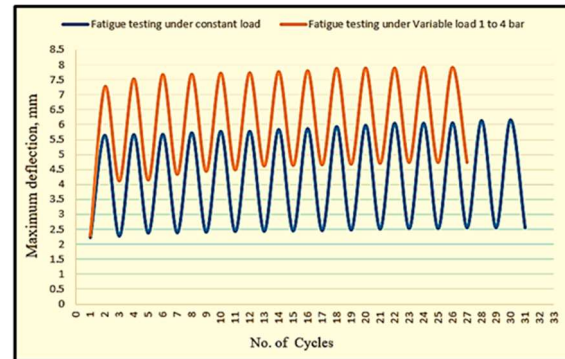


FIGURE 6. The maximum deflection of a CFRP specimen's fatigue under constant load compared to the maximum fatigue testing under variable load at pressures ranging from 1 bar to 4 bar.

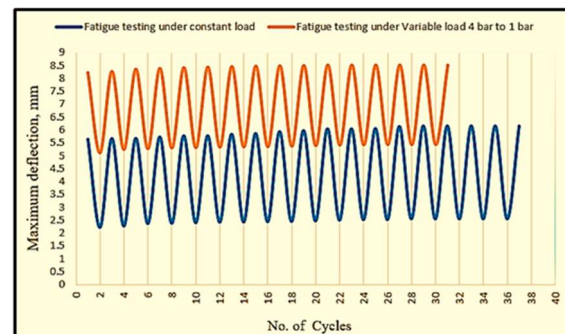


FIGURE 7. The maximum deflection of a CFRP specimen's fatigue under constant load compared to the maximum fatigue testing under variable load at pressures ranging from 4 bar to 1 bar.

* Theoretical vs. experimental outcomes

Experimental findings of sample deformation stages were compared to theoretical results, concentrating on the largest deviation from the applied load gradation in

increasing order. This study used Tables (4,5,6) to calculate the sample's produced stresses and strains. These tables provide theoretical and experimental maximum deviation, stresses, and strains. Figures (8,9,10) show the results of route diagrams for each table.

TABLE 4. CFRP's experimental and theoretical deflection in response to the applied load

Pressure *10 ⁵ N/m ²	Experimental Under Static load	Theoretical Under Static load
	Max. Deflection mm	Max. Deflection mm
1	2.30	1.68
2	3.65	3.21
3	4.84	4.74
4	5.94	6.25

The experimental findings regarding the maximum deflection demonstrated a strong correlation with the theoretical predictions for maximum deflection. The initial reading showed a notable difference between the experimental deviation and the theoretical expectation. This discrepancy in the maximum deflection can be attributed to the application of the large deflection theory, as it does not sense the slight discrepancy observed in the experimental data. The experimental and theoretical values exhibited a linear relationship concerning the sample's deformation, with the experimental results demonstrating strong convergence. This convergence supports the formulation of reliable scientific

conclusions for fatigue testing under constant load across both types. The maximum deflection values obtained from fatigue testing under constant load in this study were utilized to represent the greatest extent of deformation that the sample experiences during any of the tests, as illustrated in the comparison. Table (4) presents the maximum deflection values under static load, both experimentally and theoretically, as well as the results of fatigue testing under constant load conducted experimentally.

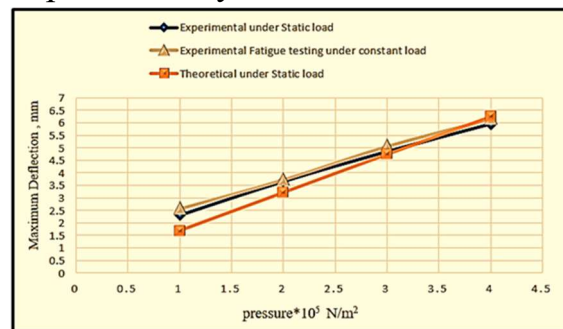


FIGURE 8. The experimental deflection of CFRP material subjected to static load and fatigue testing under constant load compared to theoretical deflection.

TABLE 5. Maximum stresses and strains for CFRP center experimental deflection under static load

Pressure *10 ⁵ N/m ²	Stress MN/m ²	Radial Strain $\epsilon_r = \epsilon_\theta$	Tangential Strain (ϵ_t)	Effective Strain (ϵ_{eff})
1	7425	0.000434485	-0.0008690	0.0008690
2	14175	0.001094221	-0.0021884	0.0021884
3	20925	0.001924023	-0.0036907	0.0037439
4	27675	0.002897960	-0.0057959	0.0057959

Table (5) the relationship between stress and strain based on the highest experimental deflection depicted in Figure (9), with this correlation remaining linear from the

initiation of loading until the peak load of ($4 \times 10^5 \text{ N/m}^2$) is attained.

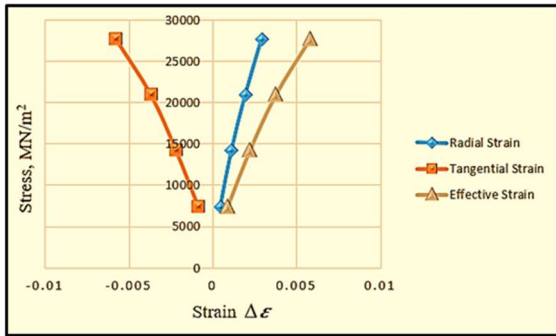


FIGURE 9. Relationship between strain and stress based on experimental results of maximum deflection of CFRP

TABLE 6. Maximum stresses and strains for CFRP center theoretical deflection under static load

Pressure $\times 10^5 \text{ N/m}^2$	Stress MN/m^2	Radial Strain $\epsilon_r = \epsilon_\theta$	Tangential Strain (ϵ_t)	Effective Strain (ϵ_{eff})
1	7425	0.000231813	-0.0004636	0.0004636
2	14175	0.000846310	-0.0016926	0.0016926
3	20925	0.001845334	-0.0036907	0.0036907
4	27675	0.003208333	-0.0064167	0.0064167

Table (6) shows the theoretical results of the strains corresponding to the stresses according to the maximum theoretical deflection, and the figure (10) their path. The agreement between the experimental and theoretical results shows a great convergence and a path similar to what is found in the experimental results in the strain mechanism in the gradation of loads imposed on the sample.

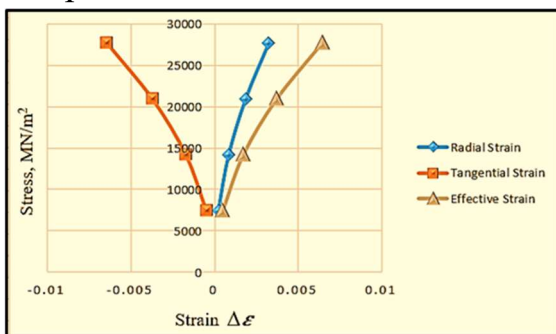


FIGURE 10. Relationship between strain and stress based on theoretical results of maximum deflection of CFRP

Figure (11) illustrates the correlation between the number of cycles and the strains induced by the loads applied to the sample during the fatigue testing under constant load, achieving its maximum value at peak loads of ($4 \times 10^5 \text{ N/m}^2$).

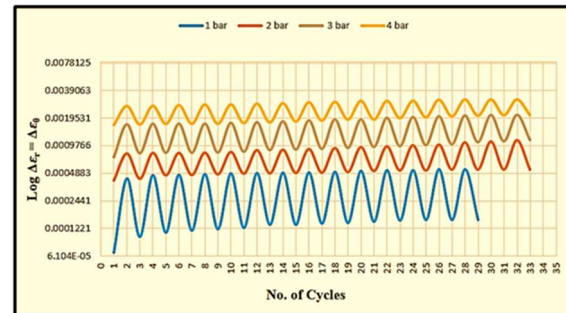


FIGURE 11. The relationship between strain and number of cycles in fatigue testing under constant load for CFRP

* CONCLUSION

The device used in the experimental test was built on solid foundations and high-precision software control of the sequence of operations and wide time range through which composite materials can be tested under different pressures and loads, whether they are regularly or unevenly graded and under static or dynamic loads in a practical and somewhat accurate manner.

The deformation phases of the specimen exhibited linear behavior throughout all tests within identical parameters, irrespective of being subjected to static loading or fatigue

testing under constant load or variable. The principal findings of this study may be encapsulated as follows: -

1- The CFRP plate exhibits reduced deformation under static load, with a maximum deflection of (5.94 mm) , compared to the fatigue test under constant load, which recorded a maximum deflection of (6.16 mm) at the highest applied pressure.

2- The fatigue testing conducted under variable loads, with pressure ranges from 1 to 4 bar, demonstrated increased deformation, achieving a maximum deflection of (7.91 mm), compared to (6.16 mm) during fatigue testing under constant load.

3- The specimen exhibits greater deformation when subjected to varying loads ranging from 4 to 1 bar compared to static load, fatigue testing under constant load, or low-to-high fatigue, achieving a maximum deflection of (8.51 mm). Initiating with high pressure provides greater impetus for deformation compared to a gradual approach or transitioning from low to high pressures.

4- The first three cycles of the low-to-high pressure test record the largest difference in maximum deflection values and specimen deformation compared to the fatigue testing under constant load, while the first and

second batches of the high-to-low Pressure test do.

5- In comparison to fatigue testing under constant load, the maximal deflection values stabilize at fewer cycles and greater deformation in both tests of fatigue under variable load.

* REFERENCES

- Mohan, N. S., Ramachandra, A., & Kulkarni, S. M. (2005). Influence of process parameters on cutting force and torque during drilling of glass-fiber polyester reinforced composites. *Composite structures*, 71(3-4), 407-413.
- Yashas Gowda, T. G., Sanjay, M. R., Subrahmanya Bhat, K., Madhu, P., SenthamaraiKannan, P., & Yogesha, B. (2018). Polymer matrix-natural fiber composites: An overview. *Cogent Engineering*, 5(1), 1446667.
- Ozcan S D, Tezcan J, Filip P. Microstructure and elastic properties of individual components of C/C composites[J]. *Carbon*, 2009, 47(15):3403-3414.
- SUN Chao, ZHANG Bo, YANG Xiao-guang, et al. Effect of cycle time of in-situ polymerisation of naphthalene

- on the densification and performance of C/C composites[J]. *New Carbon Materials*, 2012, 27(1): 49-54.
- Qin, X., Lu, Y., Xiao, H., Wen, Y., & Yu, T. (2012). A comparison of the effect of graphitization on microstructures and properties of polyacrylonitrile and mesophase pitch-based carbon fibers. *Carbon*, 50(12), 4459-4469.
- Galos, J. (2020). Thin-ply composite laminates: a review. *Composite Structures*, 236, 111920.
- G. Tang, Y. Yan, X. Chen, J. Zhang, B. Xu and Z. Feng, "Dynamic damage and fracture mechanism of three-dimensional braided carbon fiber/epoxy resin composites," *Materials and Design*, vol. 22, pp. 21-25, 2001.
- Q. Liu and M. Hughes, "The fracture behavior and toughness of woven flax fiber reinforced epoxy composites," *Composites: Part A*, vol. 39, p. 1644–1652, 2008.
- M. Arai, Y. Noro, K.-i. Sugimoto and M. Endo, "Mode I and mode II interlaminar fracture toughness of CFRP laminates toughened by carbon nanofiber interlayer," *Composites Science and Technology*, vol. 68, pp. 516-525, 2008.
- Korneeva, N., Kudinov, V., Krylov, I., & Mamonov, V. (2017). Properties of fiber reinforced plastics under static and dynamic loading conditions. *Polymer Engineering & Science*, 57(7), 693-696.
- Keller, T., & Tirelli, T. (2004). Fatigue behavior of adhesively connected pultruded GFRP profiles. *Composite structures*, 65(1), 55-64.
- Li, C., Guo, R., Xian, G., & Li, H. (2020). Effects of elevated temperature, hydraulic pressure and fatigue loading on the property evolution of a carbon/glass fiber hybrid rod. *Polymer Testing*, 90, 106761.
- Guo, R., Li, C., Niu, Y., & Xian, G. (2022). The fatigue performances of carbon fiber reinforced polymer composites—a review. *Journal of Materials Research and Technology*, 21, 4773-4789.
- Johri, N., Kandpal, B. C., Kumar, N., & Srivastava, A. (2021). Effect of ply thickness and orientation on fatigue delamination of laminated

- composites using cohesive zone model. *Materials Today: Proceedings*, 46, 11040-11045.
- Vieille, B., & Albouy, W. (2014). About the applicability of a simple model to predict the fatigue life and behavior of woven-ply thermoplastic laminates at $T > T_g$. *Composites Part B: Engineering*, 61, 181-190.
- Capela, C., Oliveira, S. E., & Ferreira, J. A. M. (2019). Fatigue behavior of short carbon fiber reinforced epoxy composites. *Composites Part B: Engineering*, 164, 191-197.
- Uusitalo, K. (2013). Designing in carbon fibre composites.
- Vassilopoulos, A. P., Keller, T., Vassilopoulos, A. P., & Keller, T. (2011). Introduction to the fatigue of fiber-reinforced polymer composites. *Fatigue of Fiber-reinforced Composites*, 1-23.
- Vassilopoulos, A. P. (2010). Introduction to the fatigue life and structures: past, present and future prospects. In *Fatigue life prediction of composites and composite structures* (pp. 1-44). Woodhead Publishing.
- Mojahedin, A., Jabbari, M., Khorshidvand, A. R., & Eslami, M. R. (2016). Buckling analysis of functionally graded circular plates made of saturated porous materials based on higher order shear deformation theory. *Thin-Walled Structures*, 99, 83-90.
- Ugural, A. C. (2009). *Stresses in beams, plates, and shells*. CRC press.
- Timoshenko, S. (1959). *Theory of plates and shells*. McGRAW HILL.
- Hosford, W. F., & Caddell, R. M. (2011). *Metal forming: mechanics and metallurgy*. Cambridge University Press.
- Khalifeh, A. (2023). Perspective Chapter: Fatigue of Materials. In *Failure Analysis-Structural Health Monitoring of Structure and Infrastructure Components*. IntechOpen.